

# A new quasi-3D HSDT for buckling and vibration of FG plate

Mohamed Sekkal<sup>1,2</sup>, Bouazza Fahsi<sup>\*2</sup>, Abdelouahed Tounsi<sup>1,2,3</sup> and S.R. Mahmoud<sup>4</sup>

<sup>1</sup>Faculty of Technology, Civil Engineering Department, Material and Hydrology Laboratory, University of Sidi Bel Abbès, Algeria

<sup>2</sup>Laboratoire de Modélisation et Simulation Multi-échelle, Département de Physique, Faculté des Sciences Exactes, Département de Physique, Université de Sidi Bel Abbès, Algeria

<sup>3</sup>Laboratoire des Structures et Matériaux Avancés dans le Génie Civil et Travaux Publics, Université de Sidi Bel Abbès, Faculté de Technologie, Département de Génie Civil, Algeria

<sup>4</sup>Department of Mathematics, Faculty of Science, King Abdulaziz University, Saudi Arabia

(Received June 14, 2017, Revised August 14, 2017, Accepted August 18, 2017)

**Abstract.** A new quasi-3D higher shear deformation theory (quasi-3D HSDT) for functionally graded plates is proposed in this article. The theory considers both shear deformation and thickness-stretching influences by a hyperbolic distribution of all displacements within the thickness, and respects the stress-free boundary conditions on the upper and lower surfaces of the plate without using any shear correction factor. The highlight of the proposed theory is that it uses undetermined integral terms in displacement field and involves a smaller number of variables and governing equations than the conventional quasi-3D theories, but its solutions compare well with 3D and quasi-3D solutions. Equations of motion are obtained from the Hamilton principle. Analytical solutions for buckling and dynamic problems are deduced for simply supported plates. Numerical results are presented to prove the accuracy of the proposed theory.

**Keywords:** buckling; vibration; sandwich plate; functionally graded materials; quasi-3D HSDT

## 1. Introduction

Functionally graded materials (FGMs) are considered as a new class of heterogeneous composite material in which the properties vary gradually over one or more directions. This material is fabricated from mixing two or more materials by considering certain volume ratio. Material characteristics of FGM vary within the material size depending on a function. Such material has been proposed, developed and successfully employed in industrial applications since 1980s (Koizumi 1993). Conventional composites structures such as fiber reinforced plastic (FRP) suffer from discontinuity of material characteristics at the interface of the plies and constituents. Hence the stress fields in these regions induce interface problems and thermal stress concentrations under high temperature environments. Furthermore, large plastic deformation of the interface may trigger the initiation and propagation of cracks in the material (Vel and Batra 2004). These problems can be reduced by gradually varying the volume fraction of constituent materials and tailoring the material for the desired application. Since its developments in the 1980s, FGMs are alternative materials widely utilized in aerospace, nuclear reactor, energy sources, biomechanical, optical, civil, automotive, electronic, chemical, mechanical, and shipbuilding industries

(Koizumi 1993, Larbi Chaht *et al.* 2015, Akbaş 2015, Arefi 2015a, b, Arefi and Allam 2015, Mahmoud *et al.*

2015, Zemri *et al.* 2015, Bousahla *et al.* 2016, Boukhari *et al.* 2016, Turan *et al.* 2016, El-Hassar *et al.* 2016, Ahouel *et al.* 2016, Benferhat *et al.* 2016, Celebi *et al.* 2016, Darabi and Vosoughi 2016, Ebrahimi and Shafiei 2016, Mohammadimehr *et al.* 2016, Mouaici *et al.* 2016, Trinh *et al.* 2016, Turan *et al.* 2016, Mouffoki *et al.* 2017).

Large applications of functionally graded (FG) structures have encouraged the development of various plate theories to study accurately their bending, stability and vibration behaviors. They are generally followed: classical plate theory (CPT) neglecting the transverse shear deformation influences (Feldman and Aboudi 1997, Javaheri and Eslami 2002, Mahdavian 2009, Mohammadi *et al.* 2010, Chen *et al.* 2006, Baferani *et al.* 2011, Arani and Kolahchi 2016, Bilouei *et al.* 2016, Zamanian *et al.* 2017), first-shear deformation theory (FSDT) with linear distribution of displacements (Mohammadi *et al.* 2010, Chen *et al.* 2006, Baferani *et al.* 2011, Praveen and Reddy 1998, Croce and Venini 2004, Efraim and Eisenberger 2007, Zhao *et al.* 2009a, b, Hosseini-Hashemi *et al.* 2011a, Naderi and Saidi 2010, Meksi *et al.* 2015, Adda Bedia *et al.* 2015, Bellifa *et al.* 2016, Boudierba *et al.* 2016, Kolahchi *et al.* 2016a, b, Hadji *et al.* 2016, Ebrahimi and Jafari 2016, Madani *et al.* 2016), higher-order shear deformation theory (HSDT) with nonlinear variations of displacements within the plate thickness such as third-order shear deformation plate theory (TSDT), sinusoidal shear deformation plate theory (SSDT), hyperbolic shear deformable plate theory (HDT), zigzag theories (Reddy 2000, Jha *et al.* 2013, Reddy 2011, Talha and Singh 2010, Tounsi *et al.* 2013, Boudierba *et al.* 2013, Ait Amar Meziane *et al.* 2014, Attia *et al.* 2015, Meradjah *et al.* 2015, Merazi *et al.* 2015, Bakora and Tounsi 2015, Mahi *et al.* 2015, Bouguenina *et al.* 2015, Ait

\*Corresponding author, Ph.D.  
E-mail: hb\_fahsi@yahoo.fr

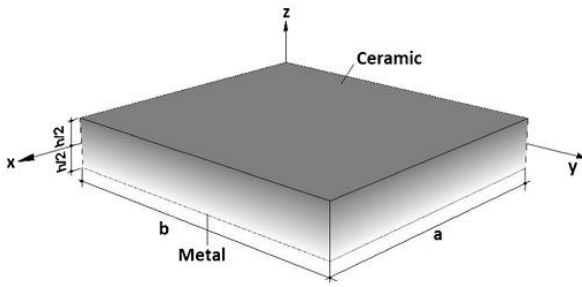


Fig. 1 Geometry of a functionally graded plate

Yahia *et al.* 2015, Bennai *et al.* 2015, Ait Atmane *et al.* 2015, Nguyen *et al.* 2015, Taibi *et al.* 2015, Zenkour 2006, Matsunaga 2008, Thai and Choi 2012, Kolahchi and Moniri Bidgoli 2016, Baseri *et al.* 2016, Chikh *et al.* 2016, Barati and Shahverdi 2016, Bourada *et al.* 2016, Merdaci *et al.* 2016, Raminnea *et al.* 2016, Saidi *et al.* 2016, Hebali *et al.* 2016, Javed *et al.* 2016, Barka *et al.* 2016, Becheri *et al.* 2016, Laoufi *et al.* 2016, Ebrahimi and Habibi, 2016, Beldjelili *et al.* 2016, El-Haina *et al.* 2017, Khetir *et al.* 2017, Klouche *et al.* 2017, Kolahchi *et al.* 2017a, b, Kolahchi, 2017, Besseghier *et al.* 2017, Chikh *et al.* 2017, Bellifa *et al.* 2017, Meksi *et al.* 2017, Zidi *et al.* 2017, Sekkal *et al.* 2017) and quasi-3D theories taking into consideration normal stretching influence (Carrera *et al.* 2008, Wu and Chiu 2011, Reddy 2011, Talha and Singh 2010, Neves *et al.* 2012a, b, Mantari and Soares 2012, 2013, Chen *et al.* 2009, Jha *et al.* 2013, Hebali *et al.* 2014, Hamidi *et al.* 2015, Akavci and Tanrikulu 2015, Pradyumna and Bandyopadhyay 2008, Bessaim *et al.* 2013, Fekrar *et al.* 2014, Kar *et al.* 2015, Swaminathan and Naveenkumar, 2014, Belabed *et al.* 2014, Bousahla *et al.* 2014, Bourada *et al.* 2015, Bounouara *et al.* 2016, Houari *et al.* 2016, Ghorbanpour Arani *et al.* 2016, Bennoun *et al.* 2016, Draiche *et al.* 2016, Benbakhti *et al.* 2016, Benchohra *et al.* 2017, Bouafia *et al.* 2017, Benahmed *et al.* 2017, Rahmani *et al.* 2017, Ait Atmane *et al.* 2017). However practically, some of these theories are computational costs because of number of additional variables included to the model (Pradyumna and Bandyopadhyay 2008, Jha *et al.* 2013, Neves *et al.* 2012a, b, Reddy 2011, Talha and Singh 2010). As a consequence, a simple quasi-3D HSDT proposed in this work is necessary.

This work aims to develop a simple quasi-3D HSDT for free vibration and buckling analysis of FG plates. By making a further assumption to the existing quasi-3D HSDT, the proposed theory contains only four unknowns and its governing equations is therefore reduced. Hamilton's principle is employed to determine equations of motion and Navier-type analytical solutions for simply-supported plates are compared with the existing solutions to check the validity of the proposed simple theory. The material properties are continuously changed within the plate thickness by the power-law form. Numerical results are found to examine the influences of the gradient index and side-to-thickness ratio on the critical buckling load and natural frequencies.

## 2. Theoretical formulation

Consider a FG plate as presented in Fig. 1 with a thickness  $h$ , length  $a$  and width  $b$ .

The material properties change across the thickness with a power law distribution, which is presented below (Zidi *et al.* 2014, 2017, Belkorissat *et al.* 2015, Fahsi *et al.* 2017)

$$P(z) = (P_c - P_m)V_c + P_m \quad (1)$$

Where  $P_c$  and  $P_m$  are the Young's moduli ( $E$ ), Poisson's ratio ( $\nu$ ) and mass density ( $\rho$ ) of ceramic and metal materials located at the upper and lower surfaces, respectively. The volume fraction of ceramic material  $V_c$  is expressed as follows

$$V_c(z) = \left( \frac{2z+h}{2h} \right)^p \quad (2)$$

Where  $p$  is the material index, which is positive.

### 2.1 Kinematics and strains

The displacement field satisfying the conditions of transverse shear stresses (and hence strains) vanishing at a point  $(x, y, \pm h/2)$  on the top and bottom surfaces of the plate, is expressed as follows

$$u(x, y, z, t) = u_0(x, y, t) - z \frac{\partial w_0}{\partial x} + k_1 f(z) \int \theta(x, y, t) dx \quad (3a)$$

$$v(x, y, z, t) = v_0(x, y, t) - z \frac{\partial w_0}{\partial y} + k_2 f(z) \int \theta(x, y, t) dy \quad (3b)$$

$$w(x, y, z, t) = w_0(x, y, t) + g(z)\theta(x, y, t) \quad (3c)$$

The coefficients  $k_1$  and  $k_2$  depends on the geometry. It can be seen that the kinematic in Eq. (3) introduces only four unknowns ( $u_0$ ,  $v_0$ ,  $w_0$  and  $\theta$ ) with considering the thickness stretching effect.

In this work, the present quasi-3D HSDT is obtained by setting

$$f(z) = -\left[ \frac{3\pi z}{2} \sec h^2 \left( \frac{1}{2} \right) \right] + \frac{3\pi}{2} h \tanh \left( \frac{z}{h} \right), \quad (4)$$

$$g(z) = \frac{2}{15} \frac{df}{dz}$$

The strain-displacement expressions, based on this formulation, are given as follows

$$\begin{Bmatrix} \varepsilon_x \\ \varepsilon_y \\ \gamma_{xy} \end{Bmatrix} = \begin{Bmatrix} \varepsilon_x^0 \\ \varepsilon_y^0 \\ \gamma_{xy}^0 \end{Bmatrix} + z \begin{Bmatrix} k_x^b \\ k_y^b \\ k_{xy}^b \end{Bmatrix} + f(z) \begin{Bmatrix} k_x^s \\ k_y^s \\ k_{xy}^s \end{Bmatrix} \quad (5)$$

$$\begin{Bmatrix} \gamma_{yz} \\ \gamma_{xz} \end{Bmatrix} = f'(z) \begin{Bmatrix} \gamma_{yz}^0 \\ \gamma_{xz}^0 \end{Bmatrix} + g(z) \begin{Bmatrix} \gamma_{yz}^1 \\ \gamma_{xz}^1 \end{Bmatrix},$$

$$\varepsilon_z = g'(z) \varepsilon_z^0$$

Where

$$\begin{Bmatrix} \varepsilon_x^0 \\ \varepsilon_y^0 \\ \gamma_{xy}^0 \end{Bmatrix} = \begin{Bmatrix} \frac{\partial u_0}{\partial x} \\ \frac{\partial v_0}{\partial x} \\ \frac{\partial u_0}{\partial y} + \frac{\partial v_0}{\partial x} \end{Bmatrix}, \quad \begin{Bmatrix} k_x^b \\ k_y^b \\ k_{xy}^b \end{Bmatrix} = \begin{Bmatrix} -\frac{\partial^2 w_0}{\partial x^2} \\ -\frac{\partial^2 w_0}{\partial y^2} \\ -2\frac{\partial^2 w_0}{\partial x \partial y} \end{Bmatrix} \quad (6a)$$

$$\begin{Bmatrix} k_x^s \\ k_y^s \\ k_{xy}^s \end{Bmatrix} = \begin{Bmatrix} k_1 \theta \\ k_2 \theta \\ k_1 \frac{\partial}{\partial y} \int \theta dx + k_2 \frac{\partial}{\partial x} \int \theta dy \end{Bmatrix} \quad (6b)$$

$$\begin{Bmatrix} \gamma_{yz}^0 \\ \gamma_{xz}^0 \end{Bmatrix} = \begin{Bmatrix} k_2 \int \theta dy \\ k_1 \int \theta dx \end{Bmatrix}, \quad \begin{Bmatrix} \gamma_{yz}^1 \\ \gamma_{xz}^1 \end{Bmatrix} = \begin{Bmatrix} \frac{\partial \theta}{\partial y} \\ \frac{\partial \theta}{\partial x} \end{Bmatrix} \quad (6c)$$

And

$$g'(z) = \frac{dg(z)}{dz} \quad (6d)$$

The integrals presented in the above equations shall be resolved by a Navier type method and can be expressed as follows:

$$\frac{\partial}{\partial y} \int \theta dx = A' \frac{\partial^2 \theta}{\partial x \partial y}, \quad \frac{\partial}{\partial x} \int \theta dy = B' \frac{\partial^2 \theta}{\partial x \partial y}, \quad (7)$$

$$\int \theta dx = A' \frac{\partial \theta}{\partial x}, \quad \int \theta dy = B' \frac{\partial \theta}{\partial y}$$

where the coefficients  $A'$  and  $B'$  are considered according to the type of solution employed, in this case via Navier method. Therefore,  $A'$ ,  $B'$ ,  $k_1$  and  $k_2$  are expressed as follows

$$A' = -\frac{1}{\alpha^2}, \quad B' = -\frac{1}{\beta^2}, \quad k_1 = -\alpha^2, \quad k_2 = -\beta^2 \quad (8)$$

Where  $\alpha$  and  $\beta$  are defined in expression (25).

The linear constitutive relations are given below

$$\begin{Bmatrix} \sigma_x \\ \sigma_y \\ \sigma_z \\ \tau_{xy} \\ \tau_{xz} \\ \tau_{yz} \end{Bmatrix} = \begin{bmatrix} C_{11} & C_{12} & C_{13} & 0 & 0 & 0 \\ C_{12} & C_{22} & C_{23} & 0 & 0 & 0 \\ C_{13} & C_{23} & C_{33} & 0 & 0 & 0 \\ 0 & 0 & 0 & C_{66} & 0 & 0 \\ 0 & 0 & 0 & 0 & C_{55} & 0 \\ 0 & 0 & 0 & 0 & 0 & C_{44} \end{bmatrix} \begin{Bmatrix} \varepsilon_x \\ \varepsilon_y \\ \varepsilon_z \\ \gamma_{xy} \\ \gamma_{xz} \\ \gamma_{yz} \end{Bmatrix} \quad (9)$$

Where  $C_{ij}$  are the three-dimensional elastic constants defined by

$$C_{11} = C_{22} = C_{33} = \frac{(1-\nu)E(z)}{(1-2\nu)(1+\nu)}, \quad (10a)$$

$$C_{12} = C_{13} = C_{23} = \frac{\nu E(z)}{(1-2\nu)(1+\nu)}, \quad (10b)$$

$$C_{44} = C_{55} = C_{66} = \frac{E(z)}{2(1+\nu)}, \quad (10c)$$

In consideration of different 10m height wind speed  $v_{10}$  and the power law exponent index  $\alpha$  results shown in Table 2, the representative upstream typhoon wind fields at different directions used as the input data for training ANN model are determined, which is shown in Tables 1-2.

## 2.1 Equations of motion

Hamilton's principle is herein employed to determine the equations of motion

$$0 = \int_0^t (\delta U + \delta V - \delta K) dt \quad (11)$$

Where  $\delta U$  is the variation of strain energy;  $\delta V$  is the variation of the external work done by external load applied to the plate; and  $\delta K$  is the variation of kinetic energy.

The variation of strain energy of the plate is expressed by

$$\delta U = \int_V \left[ \sigma_x \delta \varepsilon_x + \sigma_y \delta \varepsilon_y + \sigma_z \delta \varepsilon_z + \tau_{xy} \delta \gamma_{xy} + \tau_{yz} \delta \gamma_{yz} + \tau_{xz} \delta \gamma_{xz} \right] dV$$

$$= \int_{\Omega} \left[ N_x \delta \varepsilon_x^0 + N_y \delta \varepsilon_y^0 + N_z \delta \varepsilon_z^0 + N_{xy} \delta \gamma_{xy}^0 + M_x^b \delta k_x^b + M_y^b \delta k_y^b + M_{xy}^b \delta k_{xy}^b + M_x^s \delta k_x^s + M_y^s \delta k_y^s + M_{xy}^s \delta k_{xy}^s + Q_{yz}^s \delta \gamma_{yz}^0 + S_{yz}^s \delta \gamma_{yz}^1 + Q_{xz}^s \delta \gamma_{xz}^0 + S_{xz}^s \delta \gamma_{xz}^1 \right] dA \quad (12)$$

Where  $A$  is the top surface and the stress resultants  $N$ ,  $M$ ,  $S$  and  $Q$  are defined by

$$(N_i, M_i^b, M_i^s) = \int_{-h/2}^{h/2} (1, z, f) \sigma_i dz, \quad (i = x, y, xy), \quad (13a)$$

$$N_z = \int_{-h/2}^{h/2} g'(z) \sigma_z dz \quad (13b)$$

$$(S_{xz}^s, S_{yz}^s) = \int_{-h/2}^{h/2} g(\tau_{xz}, \tau_{yz}) dz, \quad (13c)$$

$$(Q_{xz}^s, Q_{yz}^s) = \int_{-h/2}^{h/2} f'(\tau_{xz}, \tau_{yz}) dz \quad (13d)$$

The variation of work done by in-plane loads is given by:

$$\delta V = - \int_A \bar{N} \delta w dA \quad (14)$$

With

$$\bar{N} = \left[ N_x^0 \frac{\partial^2 w}{\partial x^2} + 2N_{xy}^0 \frac{\partial^2 w}{\partial x \partial y} + N_y^0 \frac{\partial^2 w}{\partial y^2} \right] \quad (15)$$

Where  $(N_x^0, N_y^0, N_{xy}^0)$  are in-plane applied loads.

The variation of kinetic energy of the plate can be written as

$$\begin{aligned}
 \delta K &= \int_V [\dot{u} \delta \dot{u} + \dot{v} \delta \dot{v} + \dot{w} \delta \dot{w}] \rho(z) dV \\
 &= \int_A \left\{ I_0 [\dot{u}_0 \delta \dot{u}_0 + \dot{v}_0 \delta \dot{v}_0 + \dot{w}_0 \delta \dot{w}_0] \right. \\
 &\quad - I_1 \left( \dot{u}_0 \frac{\partial \delta \dot{w}_0}{\partial x} + \frac{\partial \dot{w}_0}{\partial x} \delta \dot{u}_0 + \dot{v}_0 \frac{\partial \delta \dot{w}_0}{\partial y} + \frac{\partial \dot{w}_0}{\partial y} \delta \dot{v}_0 \right) \\
 &\quad + J_1 \left[ (k_1 A') \left( \dot{u}_0 \frac{\partial \delta \dot{\theta}}{\partial x} + \frac{\partial \dot{\theta}}{\partial x} \delta \dot{u}_0 \right) \right. \\
 &\quad \left. + (k_2 B') \left( \dot{v}_0 \frac{\partial \delta \dot{\theta}}{\partial y} + \frac{\partial \dot{\theta}}{\partial y} \delta \dot{v}_0 \right) \right] \\
 &\quad + J_1^s (\dot{w}_0 \delta \dot{\theta} + \dot{\theta} \delta \dot{w}_0) \\
 &\quad + I_2 \left( \frac{\partial \dot{w}_0}{\partial x} \frac{\partial \delta \dot{w}_0}{\partial x} + \frac{\partial \dot{w}_0}{\partial y} \frac{\partial \delta \dot{w}_0}{\partial y} \right) \\
 &\quad + K_2 \left[ (k_1 A')^2 \left( \frac{\partial \dot{\theta}}{\partial x} \frac{\partial \delta \dot{\theta}}{\partial x} \right) + (k_2 B')^2 \left( \frac{\partial \dot{\theta}}{\partial y} \frac{\partial \delta \dot{\theta}}{\partial y} \right) \right] \\
 &\quad - J_2 \left[ (k_1 A') \left( \frac{\partial \dot{w}_0}{\partial x} \frac{\partial \delta \dot{\theta}}{\partial x} + \frac{\partial \dot{\theta}}{\partial x} \frac{\partial \delta \dot{w}_0}{\partial x} \right) \right. \\
 &\quad \left. + (k_2 B') \left( \frac{\partial \dot{w}_0}{\partial y} \frac{\partial \delta \dot{\theta}}{\partial y} + \frac{\partial \dot{\theta}}{\partial y} \frac{\partial \delta \dot{w}_0}{\partial y} \right) \right] \\
 &\quad \left. + K_2^s \dot{\theta} \delta \dot{\theta} \right\} dA \quad (16)
 \end{aligned}$$

Where dot-superscript convention indicates the differentiation with respect to the time variable  $t$ ;  $\rho(z)$  is the mass density given by Eq. (1); and  $(I_j, J_i, K_i)$  are mass inertias expressed by

$$(I_0, I_1, I_2) = \int_{-h/2}^{h/2} (1, z, z^2) \rho(z) dz \quad (17a)$$

$$(J_1, J_1^s, J_2, K_2, K_2^s) = \int_{-h/2}^{h/2} (f, g, z f, f^2, g^2) \rho(z) dz \quad (17b)$$

By substituting Eqs. (12), (14) and (16) into Eq. (11), the following equations of motion can be obtained

$$\begin{aligned}
 \delta u_0 : \quad & \frac{\partial N_x}{\partial x} + \frac{\partial N_{xy}}{\partial y} = I_0 \ddot{u}_0 - I_1 \frac{\partial \ddot{w}_0}{\partial x} + k_1 A' J_1 \frac{\partial \ddot{\theta}}{\partial x} \\
 \delta v_0 : \quad & \frac{\partial N_{xy}}{\partial x} + \frac{\partial N_y}{\partial y} = I_0 \ddot{v}_0 - I_1 \frac{\partial \ddot{w}_0}{\partial y} + k_2 B' J_1 \frac{\partial \ddot{\theta}}{\partial y} \\
 \delta w_0 : \quad & \frac{\partial^2 M_x}{\partial x^2} + 2 \frac{\partial^2 M_{xy}}{\partial x \partial y} + \frac{\partial^2 M_y}{\partial y^2} + N_x^0 \frac{\partial^2 w}{\partial x^2} \\
 & + 2 N_{xy}^0 \frac{\partial^2 w}{\partial x \partial y} + N_y^0 \frac{\partial^2 w}{\partial y^2} = I_0 \ddot{w}_0 + I_1 \left( \frac{\partial \ddot{u}_0}{\partial x} + \frac{\partial \ddot{v}_0}{\partial y} \right) \\
 & - I_2 \nabla^2 \ddot{w}_0 + J_2 \left( k_1 A' \frac{\partial^2 \ddot{\theta}}{\partial x^2} + k_2 B' \frac{\partial^2 \ddot{\theta}}{\partial y^2} \right) - J_1^s \ddot{\theta}
 \end{aligned}$$

$$\begin{aligned}
 \delta \theta : \quad & -k_1 A' \frac{\partial^2 S_x}{\partial x^2} - k_2 B' \frac{\partial^2 S_y}{\partial y^2} \\
 & - (k_1 A' + k_2 B') \frac{\partial^2 S_{xy}}{\partial x \partial y} + k_1 A' \frac{\partial R_{xz}}{\partial x} + k_2 B' \frac{\partial R_{yz}}{\partial y} \\
 & + g(0) \left( N_x^0 \frac{\partial^2 w}{\partial x^2} + 2 N_{xy}^0 \frac{\partial^2 w}{\partial x \partial y} + N_y^0 \frac{\partial^2 w}{\partial y^2} \right) \\
 & = -J_1 \left( k_1 A' \frac{\partial \ddot{u}_0}{\partial x} + k_2 B' \frac{\partial \ddot{v}_0}{\partial y} \right) \\
 & - K_2 \left( (k_1 A')^2 \frac{\partial^2 \ddot{\theta}}{\partial x^2} + (k_2 B')^2 \frac{\partial^2 \ddot{\theta}}{\partial y^2} \right) \\
 & + J_2 \left( k_1 A' \frac{\partial^2 \ddot{w}_0}{\partial x^2} + k_2 B' \frac{\partial^2 \ddot{w}_0}{\partial y^2} \right) - J_1^s \ddot{w}_0 - K_2^s \ddot{\theta} \quad (18)
 \end{aligned}$$

Substituting Eq. (5) into Eq. (9) and the subsequent results into Eq. (13), the stress resultants are obtained in terms of strains as following compact form

$$\begin{Bmatrix} N \\ M^b \\ M^s \end{Bmatrix} = \begin{bmatrix} A & B & B^s \\ B & D & D^s \\ B^s & D^s & H^s \end{bmatrix} \begin{Bmatrix} \varepsilon \\ k^b \\ k^s \end{Bmatrix} + \varepsilon^0 \begin{Bmatrix} L \\ L^a \\ R \end{Bmatrix}, \quad (19a)$$

$$\begin{Bmatrix} Q \\ S \end{Bmatrix} = \begin{bmatrix} F^s & X^s \\ X^s & A^s \end{bmatrix} \begin{Bmatrix} \gamma^0 \\ \gamma^1 \end{Bmatrix} \quad (19b)$$

$$\begin{aligned}
 N_z &= L(\varepsilon_x^0 + \varepsilon_y^0) + L^a(k_x^b + k_y^b) \\
 &+ R(k_x^s + k_y^s) + R^a \varepsilon_z^0 \quad (19c)
 \end{aligned}$$

In which

$$N = \{N_x, N_y, N_{xy}\}^t, \quad M^b = \{M_x^b, M_y^b, M_{xy}^b\}^t, \quad (20a)$$

$$M^s = \{M_x^s, M_y^s, M_{xy}^s\}^t,$$

$$\varepsilon = \{\varepsilon_x^0, \varepsilon_y^0, \gamma_{xy}^0\}^t, \quad k^b = \{k_x^b, k_y^b, k_{xy}^b\}^t, \quad (20b)$$

$$k^s = \{k_x^s, k_y^s, k_{xy}^s\}^t,$$

$$A = \begin{bmatrix} A_{11} & A_{12} & 0 \\ A_{12} & A_{22} & 0 \\ 0 & 0 & A_{66} \end{bmatrix}, \quad B = \begin{bmatrix} B_{11} & B_{12} & 0 \\ B_{12} & B_{22} & 0 \\ 0 & 0 & B_{66} \end{bmatrix}, \quad (20c)$$

$$D = \begin{bmatrix} D_{11} & D_{12} & 0 \\ D_{12} & D_{22} & 0 \\ 0 & 0 & D_{66} \end{bmatrix},$$

$$B^s = \begin{bmatrix} B_{11}^s & B_{12}^s & 0 \\ B_{12}^s & B_{22}^s & 0 \\ 0 & 0 & B_{66}^s \end{bmatrix}, \quad D^s = \begin{bmatrix} D_{11}^s & D_{12}^s & 0 \\ D_{12}^s & D_{22}^s & 0 \\ 0 & 0 & D_{66}^s \end{bmatrix} \quad (20d)$$

$$H^s = \begin{bmatrix} H_{11}^s & H_{12}^s & 0 \\ H_{12}^s & H_{22}^s & 0 \\ 0 & 0 & H_{66}^s \end{bmatrix},$$

$$\mathcal{Q} = \{\mathcal{Q}_{xz}^s, \mathcal{Q}_{yz}^s\}^t, \mathcal{S} = \{\mathcal{S}_{xz}^s, \mathcal{S}_{yz}^s\}^t, \gamma^0 = \{\gamma_{xz}^0, \gamma_{yz}^0\}^t, \quad (20e)$$

$$\gamma^1 = \{\gamma_{xz}^1, \gamma_{yz}^1\}^t$$

$$F^s = \begin{bmatrix} F_{55}^s & 0 \\ 0 & F_{44}^s \end{bmatrix}, X^s = \begin{bmatrix} X_{55}^s & 0 \\ 0 & X_{44}^s \end{bmatrix}, \quad (20f)$$

$$A^s = \begin{bmatrix} A_{55}^s & 0 \\ 0 & A_{44}^s \end{bmatrix}$$

$$\begin{Bmatrix} L \\ L^a \\ R \\ R^a \end{Bmatrix} = \int_z \lambda(z) \begin{Bmatrix} 1 \\ z \\ f(z) \\ g'(z) \frac{1-\nu}{\nu} \end{Bmatrix} g'(z) dz \quad (20g)$$

and stiffness components are given as

$$\begin{Bmatrix} A_{11} & B_{11} & D_{11} & B_{11}^s & D_{11}^s & H_{11}^s \\ A_{12} & B_{12} & D_{12} & B_{12}^s & D_{12}^s & H_{12}^s \\ A_{66} & B_{66} & D_{66} & B_{66}^s & D_{66}^s & H_{66}^s \end{Bmatrix} = \int_z \lambda(z) \begin{Bmatrix} 1 \\ z \\ z^2 \\ f(z) \\ f^2(z) \end{Bmatrix} \begin{Bmatrix} \frac{1-\nu}{\nu} \\ \nu \\ \frac{1-2\nu}{2\nu} \end{Bmatrix} dz \quad (21a)$$

$$\begin{pmatrix} A_{22}, B_{22}, D_{22}, B_{22}^s, D_{22}^s, H_{22}^s \end{pmatrix} = \begin{pmatrix} A_{11}, B_{11}, D_{11}, B_{11}^s, D_{11}^s, H_{11}^s \end{pmatrix} \quad (21b)$$

$$\begin{pmatrix} F_{44}^s, X_{44}^s, A_{44}^s \end{pmatrix} = \int_{-h/2}^{h/2} \frac{E(z)}{2(1+\nu)} [f'(z)]^2, f'(z)g(z), g^2(z) dz \quad (21c)$$

$$\begin{pmatrix} F_{55}^s, X_{55}^s, A_{55}^s \end{pmatrix} = \begin{pmatrix} F_{44}^s, X_{44}^s, A_{44}^s \end{pmatrix} \quad (21d)$$

By substituting Eq. (19) into Eq. (18), the equations of motion can be expressed in terms of displacements ( $u_0, v_0, w_0, \theta$ ) and the appropriate equations take the form

$$\begin{aligned} & A_{11}d_{11}u_0 + A_{66}d_{22}u_0 + (A_{12} + A_{66})d_{12}v_0 \\ & - B_{11}d_{111}w_0 - (B_{12} + 2B_{66})d_{122}w_0 \\ & + (B_{66}^s(k_1A' + k_2B') + B_{12}^sk_2B')d_{122}\theta \\ & + B_{11}^sk_1A'd_{111}\theta + Ld_1\theta = I_0\ddot{u}_0 - I_1d_1\ddot{w}_0 \\ & + J_1A'k_1d_1\ddot{\theta}, \end{aligned} \quad (22a)$$

$$\begin{aligned} & A_{22}d_{22}v_0 + A_{66}d_{11}v_0 + (A_{12} + A_{66})d_{12}u_0 \\ & - B_{22}d_{222}w_0 - (B_{12} + 2B_{66})d_{112}w_0 \\ & + (B_{66}^s(k_1A' + k_2B') + B_{12}^sk_1A')d_{112}\theta \\ & + B_{22}^sk_2B'd_{222}\theta + Ld_2\theta = I_0\ddot{v}_0 - I_1d_2\ddot{w}_0 \\ & + J_1B'k_2d_2\ddot{\theta}, \end{aligned} \quad (22b)$$

$$\begin{aligned} & B_{11}d_{111}u_0 + (B_{12} + 2B_{66})d_{122}u_0 \\ & + (B_{12} + 2B_{66})d_{112}v_0 + B_{22}d_{222}v_0 \\ & - D_{11}d_{1111}w_0 - 2(D_{12} + 2D_{66})d_{1122}w_0 \\ & - D_{22}d_{2222}w_0 + D_{11}^sk_1A'd_{1111}\theta \\ & + (D_{12}^s + 2D_{66}^s)(k_1A' + k_2B')d_{1122}\theta \\ & + D_{22}^sk_2B'd_{2222}\theta + L^a(d_{11}\theta + d_{22}\theta) + N_x^0d_{11}w \\ & + 2N_{xy}^0d_{12}w + N_y^0d_{22}w \\ & = I_0\ddot{w}_0 + I_1(d_1\ddot{u}_0 + d_2\ddot{v}_0) - I_2(d_{11}\ddot{w}_0 + d_{22}\ddot{w}_0) \\ & + J_2(k_1A'd_{11}\ddot{\theta} + k_2B'd_{22}\ddot{\theta}) + J_1^s\ddot{\theta}, \end{aligned} \quad (22c)$$

$$\begin{aligned} & -k_1A'B_{11}d_{111}u_0 - (B_{12}^sk_2B' + B_{66}^s(k_1A' + k_2B'))d_{122}u_0 \\ & - (B_{22}^sk_1A' + B_{66}^s(k_1A' + k_2B'))d_{112}v_0 - B_{22}^sk_2B'd_{222}v_0 \\ & + D_{11}^sk_1A'd_{1111}w_0 + ((D_{12}^s + 2D_{66}^s)(k_1A' + k_2B'))d_{1122}w_0 \\ & + D_{22}^sk_2B'd_{2222}w_0 - H_{11}^s(k_1A')^2d_{1111}\theta \\ & - H_{22}^s(k_2B')^2d_{2222}\theta \\ & - (2H_{12}^sk_1k_2A'B' + (k_1A' + k_2B')^2H_{66}^s)d_{1122}\theta \\ & + ((k_1A')^2F_{55}^s + 2k_1A'X_{55}^s + A_{55}^s)d_{11}\theta \\ & + ((k_2B')^2F_{44}^s + 2k_2B'X_{44}^s + A_{44}^s)d_{22}\theta \\ & - 2R(k_1A'd_{11}\theta + k_2B'd_{22}\theta) - L(d_1u_0 + d_2v_0) \\ & + L^a(d_{11}w_0 + d_{22}w_0) - R^a\theta \\ & + g(0)(N_x^0d_{11}w + 2N_{xy}^0d_{12}w + N_y^0d_{22}w) \\ & = -J_1(k_1A'd_1\ddot{u}_0 + k_2B'd_2\ddot{v}_0) \\ & + J_2(k_1A'd_{11}\ddot{w}_0 + k_2B'd_{22}\ddot{w}_0) \\ & - K_2((k_1A')^2d_{11}\ddot{\theta} + (k_2B')^2d_{22}\ddot{\theta}) + J_1^s\ddot{w}_0 + K_2^s\ddot{\theta}, \end{aligned} \quad (22c)$$

Where  $d_{ij}$ ,  $d_{ijl}$  and  $d_{ijlm}$  are the following differential operators

$$\begin{aligned} d_{ij} &= \frac{\partial^2}{\partial x_i \partial x_j}, d_{ijl} = \frac{\partial^3}{\partial x_i \partial x_j \partial x_l}, \\ d_{ijlm} &= \frac{\partial^4}{\partial x_i \partial x_j \partial x_l \partial x_m}, d_i = \frac{\partial}{\partial x_i}, (i, j, l, m = 1, 2). \end{aligned} \quad (23)$$

### 3. Close-form solutions

The Navier solution method is utilized to deduce the analytical solutions for which the displacement variables are written as product of arbitrary parameters and known trigonometric functions to respect the equations of motion and boundary conditions.

$$\begin{Bmatrix} u_0 \\ v_0 \\ w_0 \\ \theta \end{Bmatrix} = \sum_{m=1}^{\infty} \sum_{n=1}^{\infty} \begin{Bmatrix} U_{mn} e^{i\omega t} \cos(\alpha x) \sin(\beta y) \\ V_{mn} e^{i\omega t} \sin(\alpha x) \cos(\beta y) \\ W_{mn} e^{i\omega t} \sin(\alpha x) \sin(\beta y) \\ X_{mn} e^{i\omega t} \sin(\alpha x) \sin(\beta y) \end{Bmatrix} \quad (24)$$

Where  $\omega$  is the frequency of free vibration of the plate,  $\sqrt{-1}$  the imaginary unit.

With

$$\alpha = m\pi/a \text{ and } \beta = n\pi/b \quad (25)$$

Considering that the plate is subjected to in-plane compressive forces of form:  $N_x^0 = -N_0$ ,  $N_y^0 = -\gamma N_0$ ,  $N_{xy}^0 = 0$ ,  $\gamma = N_y^0/N_x^0$  (here  $\gamma$  are non-dimensional load parameter). Substituting Eq. (24) into Eq. (22), the following equation is obtained

$$\begin{bmatrix} S_{11} & S_{12} & S_{13} & S_{14} \\ S_{12} & S_{22} & S_{23} & S_{24} \\ S_{13} & S_{23} & S_{33} + \eta & S_{34} + g(0)\eta \\ S_{14} & S_{24} & S_{34} + g(0)\eta & S_{44} + [g(0)]^2 \eta \end{bmatrix} - \omega^2 \begin{bmatrix} m_{11} & 0 & m_{13} & m_{14} \\ 0 & m_{22} & m_{23} & m_{24} \\ m_{13} & m_{23} & m_{33} & m_{34} \\ m_{14} & m_{24} & m_{34} & m_{44} \end{bmatrix} \begin{Bmatrix} U_{mn} \\ V_{mn} \\ W_{mn} \\ X_{mn} \end{Bmatrix} = \begin{Bmatrix} 0 \\ 0 \\ 0 \\ 0 \end{Bmatrix} \quad (26)$$

Where

$$\begin{aligned} S_{11} &= A_{11}\alpha^2 + A_{66}\beta^2, \quad S_{12} = \alpha\beta (A_{12} + A_{66}) \\ S_{13} &= -\alpha [B_{11}\alpha^2 + (B_{12} + 2B_{66})\beta^2] \\ S_{14} &= \alpha [(k_2 B' B_{12}^s + (k_1 A' + k_2 B') B_{66}^s) \beta^2 \\ &\quad + k_1 A' B_{11}^s \alpha^2 - L] \\ S_{22} &= A_{66}\alpha^2 + A_{22}\beta^2, \quad S_{23} = -\beta [B_{22}\beta^2 + (B_{12} + 2B_{66})\alpha^2] \\ S_{24} &= \beta [(k_1 A' B_{12}^s + (k_1 A' + k_2 B') B_{66}^s) \alpha^2 \\ &\quad + k_2 B' B_{22}^s \beta^2 - L] \\ S_{33} &= D_{11}\alpha^4 + 2(D_{12} + 2D_{66})\alpha^2\beta^2 + D_{22}\beta^4 \\ S_{34} &= -k_1 A' D_{11}^s \alpha^4 - 2D_{12}^s k_2 B' \alpha^2 \beta^2 \\ &\quad - 2D_{66}^s (k_1 A' + k_2 B') \alpha^2 \beta^2 - k_2 B' D_{22}^s \beta^4 \\ &\quad + L^s (\alpha^2 + \beta^2) \\ \eta &= -N_0 (\alpha^2 + \gamma \beta^2) \\ m_{11} &= I_0, \quad m_{13} = -\alpha I_1, \quad m_{14} = J_1 k_1 A' \alpha, \quad m_{22} = I_0, \\ m_{23} &= -\beta I_1, \quad m_{24} = k_2 B' \beta J_1 \\ m_{33} &= I_0 + I_2 (\alpha^2 + \beta^2) \\ m_{34} &= -J_2 (k_1 A' \alpha^2 + k_2 B' \beta^2) + J_1^s \\ m_{44} &= K_2 [(k_1 A')^2 \alpha^2 + (k_2 B')^2 \beta^2] + K_2^s \end{aligned} \quad (27)$$

Eq. (26) is a general form for buckling and dynamic analysis of FG plates under in-plane loads. The critical buckling loads ( $N_{cr}$ ) can be determined from the stability problem  $|S_{ij}|=0$  while the free vibration problem is achieved by omitting in-plane loads.

Table 1 Material properties of metal and ceramic

Matériel	Young's modulus (GPa)	Mass density (kg/m <sup>3</sup> )	Poisson's ratio
Aluminum (Al)	70	2.702	0.3
Zirconia (ZrO <sub>2</sub> )	151	3.000	0.3
Alumina (Al <sub>2</sub> O <sub>3</sub> )	380	3.800	0.3

Table 2 Comparison of the non-dimensional fundamental frequency ( $\bar{\beta}$ ) of Al/ZrO<sub>2</sub> square plates

a/h	Theory	Material index							
		0	0.1	0.2	0.5	1	2	5	10
2	3D (Uymaz and Aydogdu 2007)	1.2589	1.2296	1.2049	1.1484	1.0913	1.0344	0.9777	0.9507
	Proposed	1.2671	1.2383	1.2135	1.1571	1.0999	1.0425	0.9841	0.9581
5	3D (Uymaz and Aydogdu 2007)	1.7748	1.7262	1.6881	1.6031	1.4764	1.4628	1.4106	1.3711
	Proposed	1.7830	1.7369	1.6983	1.6149	1.5392	1.4763	1.4176	1.3787
10	3D (Uymaz and Aydogdu 2007)	1.9339	1.8788	1.8357	1.7406	1.6583	1.5958	1.5491	1.5066
	Proposed	1.9388	1.8861	1.8424	1.7504	1.6708	1.6109	1.5575	1.5140
20	3D (Uymaz and Aydogdu 2007)	1.9570	1.9261	1.8788	1.7832	1.6999	1.6401	1.5937	1.5491
	Proposed	1.9854	1.9303	1.8849	1.7902	1.7101	1.6520	1.6012	1.5561
50	3D (Uymaz and Aydogdu 2007)	1.9974	1.9390	1.8920	1.7944	1.7117	1.6522	1.6062	1.5620
	Proposed	1.9990	1.9432	1.8973	1.8017	1.7215	1.6642	1.6143	1.5687
100	3D (Uymaz and Aydogdu 2007)	1.9974	1.9416	1.8920	1.7972	1.7117	1.6552	1.6062	1.5652
	Proposed	2.0009	1.9450	1.8990	1.8034	1.7232	1.6660	1.6162	1.5706

#### 4. Numerical results and discussion

In this section, natural frequencies and critical buckling loads of simply supported FG plates are provided and compared with existing solutions to check the accuracy of the proposed new quasi-3D HSDT. FG plates made of two material combinations of metal and ceramic: Al/ZrO<sub>2</sub> and Al/Al<sub>2</sub>O<sub>3</sub> are considered. Their material properties are presented in Table 1.

For convenience, the following non-dimensional parameters are employed

$$\begin{aligned} \bar{\omega} &= \frac{\omega a^2}{h} \sqrt{\frac{\rho_c}{E_c}}, \quad \hat{\omega} = \omega h \sqrt{\frac{\rho_c}{E_c}}, \\ \bar{\beta} &= \frac{\omega ab}{\pi^2 h} \sqrt{\frac{12(1-\nu_c^2)\rho_c}{E_c}}, \quad \bar{N}_{cr} = \frac{N_{cr} a^2}{E_m h^3}, \\ \hat{N}_{cr} &= \frac{N_{cr} a^2}{D_{11} - B_{11}^2 / A_{11}} \end{aligned} \quad (28)$$

##### 4.1 Results of free vibration analysis

Table 2 shows the comparison of the fundamental frequency of Al/ZrO<sub>2</sub> square plates obtained from the proposed quasi-3D HSDT and 3D plate model Uymaz and Aydogdu (2007).

It can be seen that the computed results agree very well with 3D solution.

Table 3 Comparison of the first three non-dimensional frequencies ( $\hat{\omega}$ ) of Al/Al<sub>2</sub>O<sub>3</sub> square plates

$a/h$	Mode ( $m,n$ )	Theory	Material index				
			0.1	0.2	0.5	1	2
	1(1,1)	Quasi-3D (Matsunaga 2008)	0.2121	0.1819	0.1640	0.1383	0.1306
		TSDT (Hosseini-Hashemi <i>et al.</i> 2011)	0.2113	0.1807	0.1631	0.1378	0.1301
		FSDT (Hosseini-Hashemi <i>et al.</i> 2011)	0.2112	0.1805	0.1631	0.1397	0.1324
		Present	0.2130	0.1834	0.1665	0.1411	0.1321
5	2(1,2)	Quasi-3D (Matsunaga 2008)	0.4658	0.4040	0.3644	0.3000	0.2790
		TSDT (Hosseini-Hashemi <i>et al.</i> 2011)	0.4623	0.3989	0.3607	0.2980	0.2771
		FSDT (Hosseini-Hashemi <i>et al.</i> 2011)	0.4618	0.3978	0.3604	0.3049	0.2856
		Present	0.4682	0.4064	0.3692	0.3052	0.2818
	3(2,2)	Quasi-3D (Matsunaga 2008)	0.6688	0.5803	0.5254	0.4284	0.3948
		TSDT (Hosseini-Hashemi <i>et al.</i> 2011)	0.6676	0.5779	0.5245	0.4405	0.4097
		FSDT (Hosseini-Hashemi <i>et al.</i> 2011)	0.6791	0.5924	0.5387	0.4388	0.4019
		Present	0.0578	0.0492	0.0443	0.0381	0.0364
	1(1,1)	Quasi-3D (Matsunaga 2008)	0.0577	0.0490	0.0442	0.0381	0.0364
		TSDT (Hosseini-Hashemi <i>et al.</i> 2011)	0.0577	0.0490	0.0442	0.0382	0.0366
		FSDT (Hosseini-Hashemi <i>et al.</i> 2011)	0.0579	0.0495	0.0450	0.0390	0.0369
		Present	0.1381	0.1180	0.1063	0.0905	0.0859
10	2(1,2)	Quasi-3D (Matsunaga 2008)	0.1377	0.1174	0.1059	0.0903	0.0856
		TSDT (Hosseini-Hashemi <i>et al.</i> 2011)	0.1376	0.1173	0.1059	0.0911	0.0867
		FSDT (Hosseini-Hashemi <i>et al.</i> 2011)	0.1385	0.1189	0.1080	0.0924	0.0869
		Present	0.2113	0.1807	0.1631	0.1378	0.1301
	3(2,2)	Quasi-3D (Matsunaga 2008)	0.2112	0.1805	0.1631	0.1397	0.1324
		TSDT (Hosseini-Hashemi <i>et al.</i> 2011)	0.2130	0.1834	0.1665	0.1411	0.1321
		FSDT (Hosseini-Hashemi <i>et al.</i> 2011)	0.0148	0.0125	0.0113	0.0098	0.0094
		Present	0.0148	0.0125	0.0113	0.0098	0.0094
20	1(1,1)	Quasi-3D (Matsunaga 2008)	0.0148	0.0126	0.0115	0.0100	0.0095
		TSDT (Hosseini-Hashemi <i>et al.</i> 2011)	0.2121	0.1819	0.1640	0.1383	0.1306
		FSDT (Hosseini-Hashemi <i>et al.</i> 2011)	0.2113	0.1807	0.1631	0.1378	0.1301
		Present	0.2112	0.1805	0.1631	0.1397	0.1324

Table 3 presents effects of the material index and thickness ratio on non-dimensional frequency of FG plate.

The results are compared with solutions of FSDT Hosseini-Hashemi *et al.* (2011b), TSDT Hosseini-Hashemi *et al.* (2011b), and quasi-3D Matsunaga (2008).

It is shown that the computed results are again found more close in many cases to 3D-quasi plate model than TSDT and FSDT.

In Table 4, non-dimensional fundamental frequencies of simply supported plate are calculated for four different

Table 4 Non-dimensional natural frequencies ( $\Omega = \omega h \sqrt{\rho_m/E_m}$ ) of Al/Al<sub>2</sub>O<sub>3</sub> functionally graded plates

$b/a$	$a/h$	$p$	Theory		
			Jin <i>et al.</i> (2014)	Mantari (2015)	Present
1	10	0	0.1135	0.1137	0.1138
		1	0.0870	0.0883	0.0884
		2	0.0789	0.0806	0.0807
		5	0.0741	0.0756	0.0756
		0	0.4169	0.4183	0.4185
	5	1	0.3222	0.3271	0.3272
		2	0.2905	0.2965	0.2966
		5	0.2676	0.2726	0.2727
	2	0	1.8470	1.8543	1.8589
		1	1.4687	1.4803	1.4836
2	10	2	1.3095	1.3224	1.3255
		5	1.1450	1.1565	1.1577
		0	0.0719	0.0719	0.0719
		1	0.0550	0.0558	0.0558
		2	0.0499	0.0510	0.0510
	5	5	0.0471	0.0480	0.0480
		0	0.2713	0.2721	0.2722
		1	0.2088	0.2121	0.2121
		2	0.1888	0.1928	0.1929
		5	0.1754	0.1789	0.1789
2	2	0	0.9570	1.3075	1.3101
		1	0.7937	1.0371	1.0390
		2	0.7149	0.9297	0.9315
		5	0.6168	0.8248	0.8253

material indexes and compared with the novel 3D exact solution proposed by Jin *et al.* (2014) and quasi-3D Mantari (2015).

The results obtained present good accuracy

Fig. 2 presents the variation of natural frequencies in terms of the material index and thickness ratio.

It can be observed from these results that the natural frequencies diminish with the increase of the material index. It is due to the fact that a higher value of  $p$  corresponds to lower value of volume fraction of the ceramic phase, and thus makes the plates become the softer ones (Nguyen 2015). Fig. 2(b) demonstrates that with an increase of the thickness ratio, the shear deformation influence becomes very effective in a relatively large region ( $b/h=30$ ).

#### 4.2 Results of buckling analysis

The buckling responses of Al/Al<sub>2</sub>O<sub>3</sub> plates are investigated by considering three types of in-plane loads: uniaxial compression ( $\gamma=0$ ), biaxial compressions ( $\gamma=1$ ) and axial compression and tension ( $\gamma=-1$ ). The computed results are given in Table 5. It can be seen that the results of present work again agree well with previous solutions HSDT Nguyen (2015) and HSDT Thai and Choi (2012).

Fig. 3 presents the critical buckling loads of rectangular plates with respect to the material index.

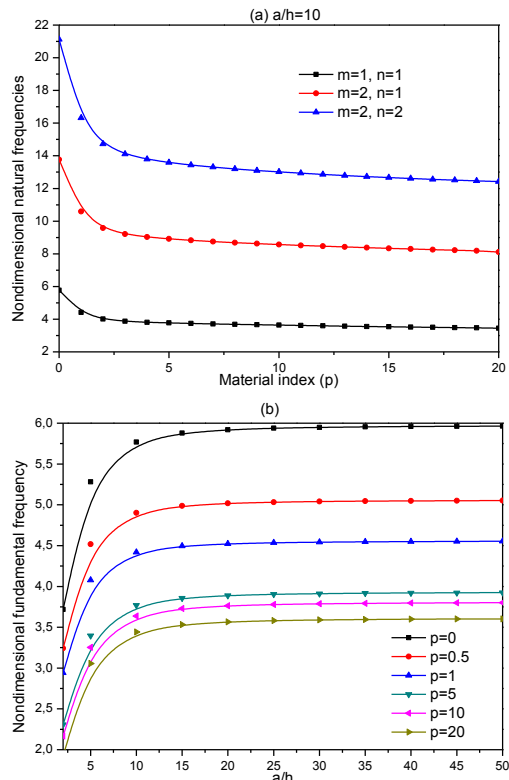


Fig. 2 Effect of the material index  $p$  and thickness ratio  $a/h$  on the natural frequency ( $\bar{\omega}$ ) of Al/Al<sub>2</sub>O<sub>3</sub> square plates

Table 5 Comparison of the critical buckling load ( $\bar{N}_{cr}$ ) of Al/Al<sub>2</sub>O<sub>3</sub> plates

$\gamma a/ba/h$	Theory	Material index					
		0	0.5	1	2	5	10
5	HSDT (Thai and Choi 2012)	6.7203	4.4235	3.4164	2.6451	2.1484	1.9213
	HSDT (Nguyen 2015)	6.7417	4.4343	3.4257	2.6503	2.1459	1.9260
	Present	6.7005	4.4728	3.4983	2.7347	2.2076	1.9459
0.5 10	HSDT (Thai and Choi 2012)	7.4053	4.8206	3.7111	2.8897	2.4165	2.1896
	HSDT (Nguyen 2015)	7.4115	4.8225	3.7137	2.8911	2.4155	2.1911
	Present	7.4126	4.8904	3.8221	3.0168	2.5090	2.2374
20	HSDT (Thai and Choi 2012)	7.5993	4.9315	3.7930	2.9582	2.4944	2.2690
	HSDT (Nguyen 2015)	7.6009	4.9307	3.7937	2.9585	2.4942	2.2695
	Present	7.6109	5.0028	3.9108	3.0968	2.5963	2.3230
0	HSDT (Thai and Choi 2012)	16.0211	10.6254	8.2245	6.3432	5.0531	4.4807
	HSDT (Nguyen, 2015)	16.1003	10.6670	8.2597	6.3631	5.0459	4.4981
	Present	15.9193	10.7065	8.3828	6.5148	5.1526	4.5077
1 10	HSDT (Thai and Choi 2012)	18.5785	12.1229	9.3391	7.2631	6.0353	5.4528
	HSDT (Nguyen 2015)	18.6030	12.1317	9.3496	7.2687	6.0316	5.4587
	Present	18.5846	12.2937	9.6083	7.5667	6.2535	5.5625
20	HSDT (Thai and Choi 2012)	19.3528	12.5668	9.6675	7.5371	6.3448	5.7668
	HSDT (Nguyen 2015)	19.3593	12.5652	9.6702	7.5386	6.3437	5.7689
	Present	19.3809	12.7494	9.9658	7.8860	6.6008	5.9020

Table 5 Continued

5	HSDT (Thai and Choi 2012)	5.3762	3.5388	2.7331	2.1161	1.7187	1.5370
	HSDT (Nguyen 2015)	5.3934	3.5475	2.7406	2.1202	1.7167	1.5408
	Present	5.3604	3.5783	2.7987	2.1878	1.7661	1.5568
0.5 10	HSDT (Thai and Choi 2012)	5.9243	3.8565	2.9689	2.3117	1.9332	1.7517
	HSDT (Nguyen 2015)	5.9292	3.8580	2.9710	2.3129	1.9324	1.7529
	Present	5.9301	3.9123	3.0577	2.4134	2.0072	1.7899
20	HSDT (Thai and Choi 2012)	6.0794	3.9452	3.0344	2.3665	1.9955	1.8152
	HSDT (Nguyen 2015)	6.0807	3.9445	3.0350	2.3668	1.9953	1.8156
	Present	6.0887	4.0022	3.1287	2.4774	2.0770	1.8584
1	HSDT (Thai and Choi 2012)	8.0105	5.3127	4.1122	3.1716	2.5265	2.2403
	HSDT (Nguyen 2015)	8.0501	5.3335	4.1299	3.1815	2.5230	2.2491
	Present	7.9597	5.3533	4.1914	3.2574	2.5763	2.2539
1 10	HSDT (Thai and Choi 2012)	9.2893	6.0615	4.6696	3.6315	3.0177	2.7264
	HSDT (Nguyen 2015)	9.3015	6.0659	4.6748	3.6344	3.0158	2.7293
	Present	9.2923	6.14687	4.8042	3.7834	3.1268	2.78123
20	HSDT (Thai and Choi 2012)	9.6764	6.2834	4.8337	3.7686	3.1724	2.8834
	HSDT (Nguyen 2015)	9.6796	6.2826	4.8351	3.7693	3.1718	2.8844
	Present	9.6904	6.3747	4.9829	3.9430	3.3004	2.9510
5	HSDT (Thai and Choi 2012)	8.9604	5.8980	4.5551	3.5268	2.8646	2.5617
	HSDT (Nguyen 2015)	8.9890	5.9124	4.5676	3.5337	2.8612	2.5679
	Present	8.9339	5.9637	4.6645	3.6463	2.9435	2.5946
10	HSDT (Thai and Choi 2012)	9.8738	6.4275	4.9481	3.8529	3.2219	2.9195
	HSDT (Nguyen 2015)	9.8820	6.4299	4.9516	3.8548	3.2206	2.9214
	Present	9.8835	6.5206	5.0962	4.0224	3.3453	3.3453
20	HSDT (Thai and Choi 2012)	10.1324	6.5753	5.0574	3.9442	3.3259	3.0253
	HSDT (Nguyen 2015)	10.1345	6.5742	5.0583	3.9447	3.3255	3.0260
	Present	10.1478	6.6704	5.2145	4.1291	3.4617	3.0974
5	HSDT (Thai and Choi 2012)	26.2058	17.7704	13.8486	10.5589	7.9590	6.8970
	HSDT (Nguyen 2015)	26.4999	17.9424	13.9872	10.6421	7.9571	6.9626
	Present <sup>a</sup>	25.7567	17.6913	13.9068	10.6372	7.9346	6.8033
10	HSDT (Thai and Choi 2012)	35.8416	23.5920	18.2206	14.1073	11.4583	10.2468
	HSDT (Nguyen 2015)	35.9559	23.6497	18.2704	14.1349	11.4447	10.2717
	Present <sup>a</sup>	35.7357	23.8550	18.6579	14.5850	11.7741	10.3784
20	HSDT (Thai and Choi 2012)	39.4951	25.7100	19.7925	15.4115	12.8878	11.6779
	HSDT (Nguyen 2015)	39.5280	25.7197	19.8065	15.4190	12.8824	11.6857
	Present <sup>a</sup>	39.5339	26.0822	20.3846	16.0896	13.3813	11.9329

<sup>a</sup> Critical buckling occurs at  $(m; n)=(2,1)$

It is seen from this figure that they diminish with the increase of the material index, and increase with the thickness ratio up to the point  $b/h=30$  from which the curves become flatter.



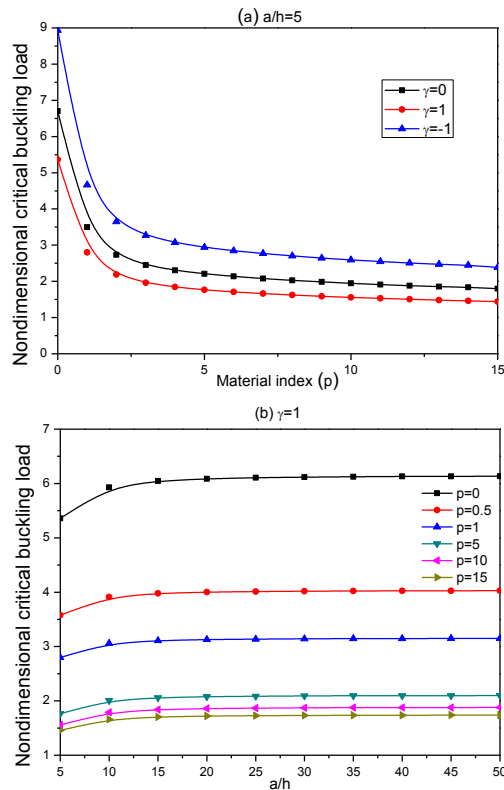


Fig. 3 Effect of the material index  $p$  and thickness ratio  $a/h$  on the critical buckling load ( $\bar{N}_{cr}$ ) of Al/Al<sub>2</sub>O<sub>3</sub> rectangular plates ( $a/b = 0.5$ )

Fig. 4 shows the lowest load-frequency curves for both homogeneous and FG rectangular plates ( $a/b=0.5$ ).

It can be observed that all fundamental frequencies decrease as in-plane loads vary from tension to compression. In compression region ( $\bar{N}_{cr} > 0$ ), the fundamental frequencies are the largest for the plates under uniaxial compression and tension ( $\gamma=-1$ ) and the smallest for ones under biaxial compressive force ( $\gamma=1$ ). However, this order is varied in tension region. It is from load-frequency curves that the critical buckling forces can be obtained indirectly by vibration investigation through load-frequency curves, which corresponds to zero natural frequencies.

## 5. Conclusions

A new quasi-3D HSDT is proposed for free vibration and buckling analysis of FG plates in this work. The theory considers hyperbolic variation of transverse shear stress, and respects the traction-free boundary conditions on the upper and lower surfaces of the plate without employing shear correction factor. The proposed plate model contains only four unknowns and equations of motion are obtained from Hamilton's principle. Navier-type solutions are determined for simply-supported plates and compared with the existing solutions to check the validity of the proposed theory. The computed results are in well agreement with different HSDTs and quasi-3D plate models. The proposed

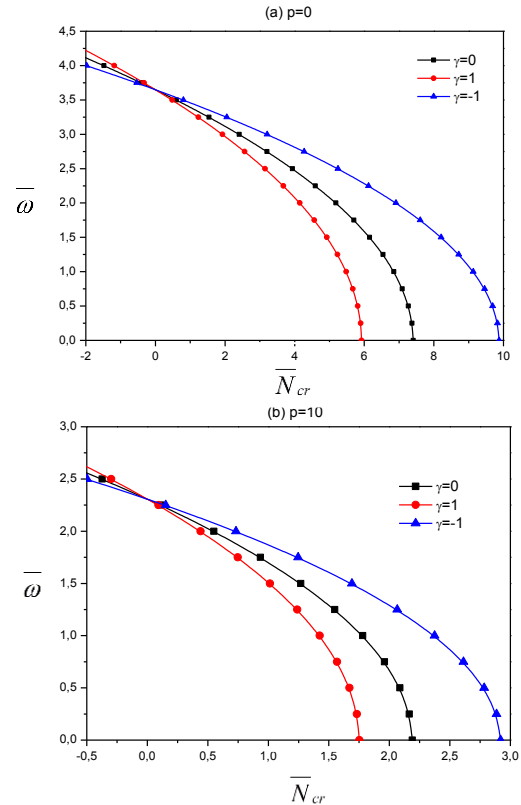


Fig. 4 Influence of in-plane loads on the non-dimensional fundamental frequency of Al/Al<sub>2</sub>O<sub>3</sub> rectangular plates ( $a/b=0.5$ ,  $a/h=10$ )

model is found to be appropriate, simple and efficient in investigating vibration and stability problem of FG plates. In addition, it is found that the proposed quasi-3D HSDT, provides results with good accuracy compared with the CPT, FSDT and other HSDTs with higher number of unknowns. Consequently, the authors suggest to consider this theory because of its simplicity.

## References

- Adda Bedia, W., Benzair, A., Semmah, A., Tounsi, A. and Mahmoud, S.R. (2015), "On the thermal buckling characteristics of armchair single-walled carbon nanotube embedded in an elastic medium based on nonlocal continuum elasticity", *Brazil. J. Phys.*, **45**(2), 225-233.
- Ahouel, M., Houari, M.S.A., Adda Bedia, E.A. and Tounsi, A. (2016) "Size-dependent mechanical behavior of functionally graded trigonometric shear deformable nanobeams including neutral surface position concept", *Steel Compos. Struct.*, **20**(5), 963-981.
- Ait Amar Meziane, M., Abdelaziz, H.H. and Tounsi, A. (2014), "An efficient and simple refined theory for buckling and free vibration of exponentially graded sandwich plates under various boundary conditions", *J. Sandw. Struct. Mater.*, **16**(3), 293-318.
- Ait Atmane, H., Tounsi, A. and Bernard, F. (2017), "Effect of thickness stretching and porosity on mechanical response of a functionally graded beams resting on elastic foundations", *Int. J. Mech. Mater. Des.*, **13**(1), 71-84.
- Ait Atmane, H., Tounsi, A., Bernard, F. and Mahmoud, S.R. (2015), "A computational shear displacement model for

- vibrational analysis of functionally graded beams with porosities", *Steel Compos. Struct.*, **19**(2), 369-384.
- Ait Yahia, S., Ait Atmane, H., Houari, M.S.A. and Tounsi, A. (2015), "Wave propagation in functionally graded plates with porosities using various higher-order shear deformation plate theories", *Struct. Eng. Mech.*, **53**(6), 1143-1165.
- Akavci, S.S. and Tanrikulu, A.H. (2015), "Static and free vibration analysis of functionally graded plates based on a new quasi-3D and 2D shear deformation theories", *Compos. Part B*, **83**, 203-215.
- Akbaş, Ş.D. (2015), "Wave propagation of a functionally graded beam in thermal environments", *Steel Compos. Struct.*, **19**(6), 1421-1447.
- Arani, A.J. and Kolahchi, R. (2016), "Buckling analysis of embedded concrete columns armed with carbon nanotubes", *Comput. Concrete*, **17**(5), 567-578.
- Arefi, M. (2015a), "Elastic solution of a curved beam made of functionally graded materials with different cross sections", *Steel Compos. Struct.*, **18**(3), 659-672.
- Arefi, M. (2015b), "Nonlinear electromechanical analysis of a functionally graded square plate integrated with smart layers resting on Winkler-Pasternak foundation", *Smart Struct. Syst.*, **16**(1), 195-211.
- Arefi, M. and Allam, M.N.M. (2015), "Nonlinear responses of an arbitrary FGP circular plate resting on the Winkler-Pasternak foundation", *Smart Struct. Syst.*, **16**(1), 81-100.
- Attia, A., Tounsi, A., Adda Bedia, E.A. and Mahmoud, S.R. (2015), "Free vibration analysis of functionally graded plates with temperature-dependent properties using various four variable refined plate theories", *Steel Compos. Struct.*, **18**(1), 187-212.
- Baferani, A.H., Saidi, A.R. and Jomehzadeh, E. (2011), "An exact solution for free vibration of thin functionally graded rectangular plates", *Proc. Inst. Mech. Eng. Part C: J. Mech. Eng. Sci.*, **225**, 526-536.
- Bakora, A. and Tounsi, A. (2015), "Thermo-mechanical post-buckling behavior of thick functionally graded plates resting on elastic foundations", *Struct. Eng. Mech.*, **56**(1), 85-106.
- Barati, M.R. and Shahverdi, H. (2016), "A four-variable plate theory for thermal vibration of embedded FG nanoplates under non-uniform temperature distributions with different boundary conditions", *Struct. Eng. Mech.*, **60**(4), 707-727.
- Barka, M., Benrahou, K.H., Bakora, A. and Tounsi, A. (2016), "Thermal post-buckling behavior of imperfect temperature-dependent sandwich FGM plates resting on Pasternak elastic foundation", *Steel Compos. Struct.*, **22**(1), 91-112.
- Baseri, V., Jafari, G.S. and Kolahchi, R. (2016), "Analytical solution for buckling of embedded laminated plates based on higher order shear deformation plate theory", *Steel Compos. Struct.*, **21**(4), 883-919.
- Becheri, T., Amara, K., Bouazza, M. and Benseddiq, N. (2016), "Buckling of symmetrically laminated plates using nth-order shear deformation theory with curvature effects", *Steel Compos. Struct.*, **21**(6), 1347-1368.
- Belabed, Z., Houari, M.S.A., Tounsi, A., Mahmoud, S.R. and Anwar Bég, O. (2014), "An efficient and simple higher order shear and normal deformation theory for functionally graded material (FGM) plates", *Compos. Part B*, **60**, 274-283.
- Beldjelili, Y., Tounsi, A. and Mahmoud, S.R. (2016), "Hygro-thermo-mechanical bending of S-FGM plates resting on variable elastic foundations using a four-variable trigonometric plate theory", *Smart Struct. Syst.*, **18**(4), 755-786.
- Belkorissat, I., Houari, M.S.A., Tounsi, A., Adda Bedia, E.A. and Mahmoud, S.R. (2015), "On vibration properties of functionally graded nano-plate using a new nonlocal refined four variable model", *Steel Compos. Struct.*, **18**(4), 1063-1081.
- Bellifa, H., Benrahou, K.H., Bousahla, A.A., Tounsi, A. and Mahmoud, S.R. (2017), "A nonlocal zeroth-order shear deformation theory for nonlinear postbuckling of nanobeams", *Struct. Eng. Mech.*, **62**(6), 695-702.
- Bellifa, H., Benrahou, K.H., Hadji, L., Houari, M.S.A. and Tounsi, A. (2016), "Bending and free vibration analysis of functionally graded plates using a simple shear deformation theory and the concept the neutral surface position", *J. Braz. Soc. Mech. Sci. Eng.*, **38**(1), 265-275.
- Benahmed, A., Houari, M.S.A., Benyoucef, S., Belakhdar, K. and Tounsi, A. (2017), "A novel quasi-3D hyperbolic shear deformation theory for functionally graded thick rectangular plates on elastic foundation", *Geomech. Eng.*, **12**(1), 9-34.
- Benbakhti, A., Bachir Bouiadjra, M., Retiel, N. and Tounsi, A. (2016), "A new five unknown quasi-3D type HSDT for thermomechanical bending analysis of FGM sandwich plates", *Steel Compos. Struct.*, **22**(5), 975-999.
- Benchohra, M., Driz, H., Bakora, A., Tounsi, A., Adda Bedia, E.A. and Mahmoud, S.R. (2017), "A new quasi-3D sinusoidal shear deformation theory for functionally graded plates", *Struct. Eng. Mech.* (in Press)
- Benferhat, R., Hassaine Daouadji, T., Hadji, L. and Said Mansour, M. (2016), "Static analysis of the FGM plate with porosities", *Steel Compos. Struct.*, **21**(1), 123-136.
- Bennai, R., Ait Atmane, H. and Tounsi, A. (2015), "A new higher-order shear and normal deformation theory for functionally graded sandwich beams", *Steel Compos. Struct.*, **19**(3), 521-546.
- Bennoun, M., Houari, M.S.A. and Tounsi, A. (2016), "A novel five variable refined plate theory for vibration analysis of functionally graded sandwich plates", *Mech. Adv. Mater. Struct.*, **23**(4), 423-431.
- Bessaim, A., Houari, M.S.A., Tounsi, A., Mahmoud, S.R. and Adda Bedia, E.A. (2013), "A new higher order shear and normal deformation theory for the static and free vibration analysis of sandwich plates with functionally graded isotropic face sheets", *J. Sandw. Struct. Mater.*, **15**, 671-703.
- Bessegghier, A., Houari, M.S.A., Tounsi, A. and Mahmoud, S.R. (2017), "Free vibration analysis of embedded nanosize FG plates using a new nonlocal trigonometric shear deformation theory", *Smart Struct. Syst.*, **19**(6), 601-614.
- Bilouei, B.S., Kolahchi, R. and Bidgoli, M.R. (2016), "Buckling of concrete columns retrofitted with Nano-Fiber Reinforced Polymer (NFRP)", *Comput. Concrete*, **18**(5), 1053-1063.
- Bouafia, K., Kaci, A., Houari, M.S.A., Benzair, A. and Tounsi, A. (2017), "A nonlocal quasi-3D theory for bending and free flexural vibration behaviors of functionally graded nanobeams", *Smart Struct. Syst.*, **19**(2), 115-126.
- Bouderba, B., Houari, M.S.A. and Tounsi, A. (2013), "Thermomechanical bending response of FGM thick plates resting on Winkler-Pasternak elastic foundations", *Steel Compos. Struct.*, **14**(1), 85-104.
- Bouderba, B., Houari, M.S.A., Tounsi, A. and Mahmoud, S.R. (2016), "Thermal stability of functionally graded sandwich plates using a simple shear deformation theory", *Struct. Eng. Mech.*, **58**(3), 397-422.
- Bouguenina, O., Belakhdar, K., Tounsi, A. and Adda Bedia, E.A. (2015), "Numerical analysis of FGM plates with variable thickness subjected to thermal buckling", *Steel Compos. Struct.*, **19**(3), 679-695.
- Boukhari, A., Ait Atmane, H., Tounsi, A., Adda Bedia, E.A. and Mahmoud, S.R. (2016), "An efficient shear deformation theory for wave propagation of functionally graded material plates", *Struct. Eng. Mech.*, **57**(5), 837-859.
- Bounouara, F., Benrahou, K.H., Belkorissat, I. and Tounsi, A. (2016), "A nonlocal zeroth-order shear deformation theory for free vibration of functionally graded nanoscale plates resting on elastic foundation", *Steel Compos. Struct.*, **20**(2), 227-249.

- Bourada, F., Amara, K. and Tounsi, A. (2016), "Buckling analysis of isotropic and orthotropic plates using a novel four variable refined plate theory", *Steel Compos. Struct.*, **21**(6), 1287-1306.
- Bourada, M., Kaci, A., Houari, M.S.A. and Tounsi, A. (2015), "A new simple shear and normal deformations theory for functionally graded beams", *Steel Compos. Struct.*, **18**(2), 409-423.
- Bousahla, A.A., Benyoucef, S., Tounsi, A. and Mahmoud, S.R. (2016), "On thermal stability of plates with functionally graded coefficient of thermal expansion", *Struct. Eng. Mech.*, **60**(2), 313-335.
- Bousahla, A.A., Houari, M.S.A., Tounsi, A. and Adda Bedia, E.A. (2014), "A novel higher order shear and normal deformation theory based on neutral surface position for bending analysis of advanced composite plates", *Int. J. Comput. Meth.*, **11**(6), 1350082.
- Carrera, E., Brischetto, S. and Robaldo, A. (2008), "Variable kinematic model for the analysis of functionally graded material plates", *AIAA J.*, **46**(1), 194-203.
- Celebi, K., Yarpapabuc, D. and Keles, I. (2016), "A unified method for stresses in FGM sphere with exponentially-varying properties", *Struct. Eng. Mech.*, **57**(5), 823-835.
- Chen, C., Hsu, C. and Tzou, G. (2009), "Vibration and stability of functionally graded plates based on a higher-order deformation theory", *J. Reinf. Plast. Compos.*, **28**, 1215-1234.
- Chen, C.S., Chen, T.J. and Chien, R.D. (2006), "Nonlinear vibration of initially stressed functionally graded plates", *Thin Wall. Struct.*, **44**(8), 844-851.
- Chikh, A., Bakora, A., Heireche, H., Houari, M.S.A., Tounsi, A. and Adda Bedia, E.A. (2016), "Thermo-mechanical postbuckling of symmetric S-FGM plates resting on Pasternak elastic foundations using hyperbolic shear deformation theory", *Struct. Eng. Mech.*, **57**(4), 617-639.
- Chikh, A., Tounsi, A., Hebali, H. and Mahmoud, S.R. (2017), "Thermal buckling analysis of cross-ply laminated plates using a simplified HSDT", *Smart Struct. Syst.*, **19**(3), 289-297.
- Croce, L.D. and Venini, P. (2004), "Finite elements for functionally graded Reissner-Mindlin plates", *Comput. Meth. Appl. Mech. Eng.*, **193**, 705-725.
- Darabi, A. and Vosoughi, A.R. (2016), "hybrid inverse method for small scale parameter estimation of FG nanobeams", *Steel Compos. Struct.*, **20**(5), 1119-1131.
- Draiche, K., Tounsi, A. and Mahmoud, S.R. (2016), "A refined theory with stretching effect for the flexure analysis of laminated composite plates", *Geomech. Eng.*, **11**(5), 671-690.
- Ebrahimi, F. and Habibi, S. (2016), "Deflection and vibration analysis of higher-order shear deformable compositionally graded porous plate", *Steel Compos. Struct.*, **20**(1), 205-225.
- Ebrahimi, F. and Jafari, A. (2016), "Thermo-mechanical vibration analysis of temperature- dependent porous FG beams based on Timoshenko beam theory", *Struct. Eng. Mech.*, **59**(2), 343-371.
- Ebrahimi, F. and Shafiei, N. (2016), "Application of Eringen's nonlocal elasticity theory for vibration analysis of rotating functionally graded nanobeams", *Smart Struct. Syst.*, **17**(5), 837-857.
- Efrain, E. and Eisenberger, M. (2007), "Exact vibration analysis of variable thickness thick annular isotropic and FGM plates", *J. Sound Vib.*, **299**, 720-738.
- El-Haina, F., Bakora, A., Bousahla, A.A., Tounsi, A. and Mahmoud, S.R. (2017), "A simple analytical approach for thermal buckling of thick functionally graded sandwich plates", *Struct. Eng. Mech.*, **63**(5), 585-595.
- El-Hassar, S.M., Benyoucef, S., Heireche, H. and Tounsi, A. (2016), "Thermal stability analysis of solar functionally graded plates on elastic foundation using an efficient hyperbolic shear deformation theory", *Geomech. Eng.*, **10**(3), 357-386.
- Fahsi, A., Tounsi, A., Hebali, H., Chikh, A., Adda Bedia, E.A. and Mahmoud, S.R. (2017), "A four variable refined  $n$ th-order shear deformation theory for mechanical and thermal buckling analysis of functionally graded plates", *Geomech. Eng.*, **13**(3), 385-410.
- Fekrar, A., Houari, M.S.A., Tounsi, A. and Mahmoud, S.R. (2014), "A new five-unknown refined theory based on neutral surface position for bending analysis of exponential graded plates", *Meccanica*, **49**, 795-810.
- Feldman, E. and Aboudi, J. (1997), "Buckling analysis of functionally graded plates subjected to uniaxial loading", *Compos. Struct.*, **38**, 29-36.
- Ghorbanpour Arani, A., Cheraghbak, A. and Kolahchi, R. (2016), "Dynamic buckling of FGM viscoelastic nano-plates resting on orthotropic elastic medium based on sinusoidal shear deformation theory", *Struct. Eng. Mech.*, **60**(3), 489-505.
- Hadji, L., Hassaine Daouadji, T., Ait Amar Meziane, M., Tlidji, Y. and Adda Bedia, E.A. (2016), "Analysis of functionally graded beam using a new first-order shear deformation theory", *Struct. Eng. Mech.*, **57**(2), 315-325.
- Hamidi, A., Houari, M.S.A., Mahmoud, S.R. and Tounsi, A. (2015), "A sinusoidal plate theory with 5-unknowns and stretching effect for thermomechanical bending of functionally graded sandwich plates", *Steel Compos. Struct.*, **18**(1), 235-253.
- Hebali, H., Bakora, A., Tounsi, A. and Kaci, A. (2016), "A novel four variable refined plate theory for bending, buckling, and vibration of functionally graded plates", *Steel Compos. Struct.*, **22**(3), 473-495.
- Hebali, H., Tounsi, A., Houari, M.S.A., Bessaim, A. and Adda Bedia, E.A. (2014), "A new quasi-3D hyperbolic shear deformation theory for the static and free vibration analysis of functionally graded plates", *ASCE J. Eng. Mech.*, **140**, 374-383.
- Hosseini-Hashemi, S., Fadaee, M. and Atashipour, S. (2011b), "Study on the free vibration of thick functionally graded rectangular plates according to a new exact closed-form procedure", *Compos. Struct.*, **93**(2), 722-735.
- Hosseini-Hashemi, S., Fadaee, M. and Atashipour, S.R. (2011a), "A new exact analytical approach for free vibration of Reissner-Mindlin functionally graded rectangular plates", *Int. J. Mech. Sci.*, **53**, 11-22.
- Houari, M.S.A., Tounsi, A., Bessaim, A. and Mahmoud, S.R. (2016), "A new simple three -unknown sinusoidal shear deformation theory for functionally graded plates", *Steel Compos. Struct.*, **22**(2), 257-276.
- Javaheri, R. and Eslami, M. (2002), "Buckling of functionally graded plates under in-plane compressive loading", *J. Appl. Math. Mech.*, **82**, 277-283.
- Javed, S., Viswanathan, K.K., Aziz, Z.A., Karthik, K. and Lee, J.H. (2016), "Vibration of antisymmetric angle-ply laminated plates under higher order shear theory", *Steel Compos. Struct.*, **22**(6), 1281-1299.
- Jha, D.K., Kant, T. and Singh, R.K. (2013), "Free vibration response of functionally graded thick plates with shear and normal deformations effects", *Compos. Struct.*, **96**, 799-823.
- Jin, G., Su, Z., Shi, S., Ye, T. and Gao, S. (2014), "Three-dimensional exact solution for the free vibration of arbitrarily thick functionally graded rectangular plates with general boundary conditions", *Compos. Struct.*, **108**, 565-577.
- Kar, V.R., Mahapatra, T.R. and Panda, S.K. (2015), "Nonlinear flexural analysis of laminated composite flat panel under hygro-thermo-mechanical loading", *Steel Compos. Struct.*, **19**(4), 1011-1033.
- Khetir, H., Bachir Bouiadja, M., Houari, M.S.A., Tounsi, A. and Mahmoud, S.R. (2017), "A new nonlocal trigonometric shear deformation theory for thermal buckling analysis of embedded nanosize FG plates", *Struct. Eng. Mech.* (in Press).
- Klouche, F., Darcherif, L., Sekkal, M., Tounsi, A. and Mahmoud,

- S.R. (2017), "An original single variable shear deformation theory for buckling analysis of thick isotropic plates", *Struct. Eng. Mech.*, **63**(4), 439-446.
- Koizumi, M. (1993), "The concept of FGM Ceramic transactions", *Funct. Grad. Mater.*, **34**, 3-10.
- Koizumi, M. (1993), "The concept of FGM ceramic transactions", *Funct. Grad. Mater.*, **34**, 3-10.
- Kolahchi, R. (2017), "A comparative study on the bending, vibration and buckling of viscoelastic sandwich nano-plates based on different nonlocal theories using DC, HDQ and DQ methods", *Aerosp. Sci. Technol.*, **66**, 235-248.
- Kolahchi, R. and Moniri Bidgoli, A.M. (2016), "Size-dependent sinusoidal beam model for dynamic instability of single-walled carbon nanotubes", *Appl. Math. Mech.*, **37**(2), 265-274.
- Kolahchi, R., Hosseini, H. and Esmailpour, M. (2016a), "Differential cubature and quadrature-Bolotin methods for dynamic stability of embedded piezoelectric nanoplates based on visco-nonlocal-piezoelectricity theories", *Compos. Struct.*, **157**, 174-186.
- Kolahchi, R., Safari, M. and Esmailpour, M. (2016b), "Dynamic stability analysis of temperature-dependent functionally graded CNT-reinforced visco-plates resting on orthotropic elastomeric medium", *Compos. Struct.*, **150**, 255-265.
- Kolahchi, R., Zarei, M.S., Hajmohammad, M.H. and Nouri, A. (2017b), "Wave propagation of embedded viscoelastic FG-CNT-reinforced sandwich plates integrated with sensor and actuator based on refined zigzag theory", *Int. J. Mech. Sci.*, **130**, 534-545.
- Kolahchi, R., Zarei, M.S., Hajmohammad, M.H. and Oskoue, A.N. (2017a), "Visco-nonlocal-refined Zigzag theories for dynamic buckling of laminated nanoplates using differential cubature-Bolotin methods", *Thin Wall. Struct.*, **113**, 162-169.
- Laoufi, I., Ameer, M., Zidi, M., Adda Bedia, E.A. and Bousahla, A.A. (2016), "Mechanical and hygrothermal behaviour of functionally graded plates using a hyperbolic shear deformation theory", *Steel Compos. Struct.*, **20**(4), 889-912.
- Larbi Chaht, F., Kaci, A., Houari, M.S.A., Tounsi, A., Anwar Bég, O. and Mahmoud, S.R. (2015), "Bending and buckling analyses of functionally graded material (FGM) size-dependent nanoscale beams including the thickness stretching effect", *Steel Compos. Struct.*, **18**(2), 425-442.
- Madani, H., Hosseini, H. and Shokravi, M. (2016), "Differential cubature method for vibration analysis of embedded FG-CNT-reinforced piezoelectric cylindrical shells subjected to uniform and non-uniform temperature distributions", *Steel Compos. Struct.*, **22**(4), 889-913.
- Mahdavian, M. (2009), "Buckling analysis of simply-supported functionally graded rectangular plates under non-uniform in-plane compressive loading", *J. Solid. Mech.*, **1**, 213-225.
- Mantari, J.L. (2015), "A refined theory with stretching effect for the dynamics analysis of advanced composites on elastic foundation", *Mech. Mater.*, **86**, 31-43.
- Mantari, J.L. and Soares, C.G. (2012), "Generalized hybrid quasi-3D shear deformation theory for the static analysis of advanced composite plates", *Compos. Struct.*, **94**(8), 2561-2575.
- Mantari, J.L. and Soares, C.G. (2013), "A novel higher-order shear deformation theory with stretching effect for functionally graded plates", *Compos. Part B: Eng.*, **45**(1), 268-281.
- Matsunaga, H. (2008), "Free vibration and stability of functionally graded plates according to a 2D higher-order deformation theory", *Compos. Struct.*, **82**, 499-512.
- Meksi, A., Benyoucef, S., Houari, M.S.A. and Tounsi, A. (2015), "A simple shear deformation theory based on neutral surface position for functionally graded plates resting on Pasternak elastic foundations", *Struct. Eng. Mech.*, **53**(6), 1215-1240.
- Mohammadi, M., Saidi, A. and Jomehzadeh, E. (2010), "Levy solution for buckling analysis of functionally graded rectangular plates", *Appl. Compos. Mater.*, **17**, 81-93.
- Naderi, A. and Saidi, A. (2010), "On pre-buckling configuration of functionally graded Mindlin rectangular plates", *Mech. Res. Commun.*, **37**, 535-538.
- Neves, A.M.A., Ferreira, A.J.M., Carrera, E., Cinefra, M., Roque, C.M.C., Jorge, R.M.N. and Soares, C.M.M. (2012a), "A quasi-3D hyperbolic shear deformation theory for the static and free vibration analysis of functionally graded plates", *Compos. Struct.*, **94**, 1814-1825.
- Neves, A.M.A., Ferreira, A.J.M., Carrera, E., Roque, C.M.C., Cinefra, M., Jorge, R.M.N. and Soares, C.M.M. (2012b), "A quasi-3D sinusoidal shear deformation theory for the static and free vibration analysis of functionally graded plates", *Compos. Part B: Eng.*, **43**, 711-725.
- Nguyen, T.K. (2015), "A higher-order hyperbolic shear deformation plate model for analysis of functionally graded materials", *Int. J. Mech. Mater. Des.*, **11**(2), 203-219.
- Pradyumna, S. and Bandyopadhyay, J.N. (2008), "Free vibration analysis of functionally graded curved panels using a higher-order finite element formulation", *J. Sound Vib.*, **318**, 176-192.
- Praveen, G.N. and Reddy, J.N. (1998), "Nonlinear transient thermoelastic analysis of functionally graded ceramic-metal plates", *Int. J. Solid. Struct.*, **35**, 4457-4476.
- Rahmani, O., Refaiejad, V. and Hosseini, S.A.H. (2017), "Assessment of various nonlocal higher order theories for the bending and buckling behavior of functionally graded nanobeams", *Steel Compos. Struct.*, **23**(3), 339-350.
- Reddy, J.N. (2000), "Analysis of functionally graded plates", *Int. J. Numer. Meth. Eng.*, **47**, 663-684.
- Reddy, J.N. (2011), "A general nonlinear third-order theory of functionally graded plates", *Int. J. Aerosp. Lightw. Struct.*, **1**, 1-21.
- Swaminathan, K. and Naveenkumar, D.T. (2014), "Higher order refined computational models for the stability analysis of FGM plates: Analytical solutions", *Eur. J. Mech. A/Solid.*, **47**, 349-361.
- Taibi, F.Z., Benyoucef, S., Tounsi, A., Bachir Bouiadjra, R., Adda Bedia, E.A. and Mahmoud, S.R. (2015), "A simple shear deformation theory for thermo-mechanical behaviour of functionally graded sandwich plates on elastic foundations", *J. Sandw. Struct. Mater.*, **17**(2), 99-129.
- Talha, M. and Singh, B.N. (2010), "Static response and free vibration analysis of FGM plates using higher order shear deformation theory", *Appl. Math. Model.*, **34**, 3991-4011.
- Thai, H.T. and Choi, D.H. (2012), "An efficient and simple refined theory for buckling analysis of functionally graded plates", *Appl. Math. Model.*, **36**, 1008-1022.
- Tounsi, A., Houari, M.S.A., Benyoucef, S. and Adda Bedia, E.A. (2013), "A refined trigonometric shear deformation theory for thermoelastic bending of functionally graded sandwich plates", *Aerosp. Sci. Tech.*, **24**, 209-220.
- Turan, M., Adiyaman, G., Kahya, V. and Birinci, A. (2016), "Axisymmetric analysis of a functionally graded layer resting on elastic substrate", *Struct. Eng. Mech.*, **58**(3), 423-442.
- Uymaz, B. and Aydogdu, M. (2007), "Three-dimensional vibration analyses of functionally graded plates under various boundary conditions", *J. Reinf. Plast. Compos.*, **26**(18), 1847-1863.
- Vel, S.S. and Batra, R.C. (2004), "Three-dimensional exact solution for the vibration of functionally graded rectangular plate", *J Sound Vib*, **272**, 703-730.
- Wu, C.P. and Chiu, K.H. (2011), "RMVT-based meshless collocation and element-free Galerkin methods for the quasi-3D free vibration analysis of multilayered composite and FGM plates", *Compos. Struct.*, **93**(5), 1433-1448.
- Zamanian, M., Kolahchi, R. and Bidgoli, M.R. (2017), "Agglomeration effects on the buckling behaviour of embedded concrete columns reinforced with SiO<sub>2</sub> nano-particles", *Wind*

- Struct.*, **24**(1), 43-57.
- Zenkour, A.M. (2006), "Generalized shear deformation theory for bending analysis of functionally graded materials", *Appl. Math. Model.*, **30**, 67-84.
- Zhao, X., Lee, Y.Y. and Liew, K.M. (2009a), "Mechanical and thermal buckling analysis of functionally graded plates", *Compos. Struct.*, **90**, 161-171.
- Zhao, X., Lee, Y.Y. and Liew, K.M. (2009b), "Free vibration analysis of functionally graded plates using the element-free kp-Ritz method", *J. Sound Vib.*, **319**, 918-939.
- Zidi, M., Houari, M.S.A., Tounsi, A., Bessaim, A. and Mahmoud, S.R. (2017), "A novel simple two-unknown hyperbolic shear deformation theory for functionally graded beams", *Struct. Eng. Mech.*, **64**(2), 145-153.
- Zidi, M., Tounsi, A., Houari, M.S.A., Adda Bedia, E.A. and Anwar Bég, O. (2014), "Bending analysis of FGM plates under hygro-thermo-mechanical loading using a four variable refined plate theory", *Aerosp. Sci. Tech.*, **34**, 24-34.